Embankment dam seepage evaluation from resistivity monitoring data

Sjödahl, Pontus; Dahlin, Torleif; Johansson, S.

Published in:
Near Surface Geophysics

2009

Near Surface Geophysics, 2009, 463-474

Embankment dam seepage evaluation from resistivity monitoring data

P. Sjödahl[1*], T. Dahlin[2] and S. Johansson[1]

[1] *HydroResearch Sam Johansson AB, Stora Marknadsvägen 15 S, 18334 Täby, Sweden*
[2] *Department of Engineering Geology, Lund University, PO Box 118, 22100 Lund, Sweden*

Received October 2008, revision accepted April 2009

ABSTRACT

Methods for monitoring seepage are important for the safety of embankment dams. Increased seepage may be associated with internal erosion in the dam and internal erosion is one of the main reasons for dam failures. Internal erosion progresses inside the dam and is difficult to detect by conventional methods. Therefore there is a need for new or improved methods. The resistivity method is a non-destructive method that may accomplish this task. It has been tried in an on-going research programme in Sweden. Daily resistivity measurements are carried out on permanent installations on two Swedish embankment dams. In this paper the installations on the Sädva embankment dam are described and selected parts of the results are presented. In addition, a method for evaluating the seepage from resistivity monitoring data is theoretically described and tested for four selected areas in the foundation of the Sädva dam. Seasonal resistivity variations are apparent in the reservoir as well as inside the dam. Most parts of the dam have a homogeneous resistivity distribution with consistent variations. The overall status of the dam is satisfactory. However part of the foundation demonstrates a slightly different behaviour pattern with regard to the seasonal variation. The four selected areas represent localities with low, intermediate and high variations in seasonal resistivity. The areas are compared qualitatively and thereby permeable zones within the dam may be identified. Quantitative assessment of the seepage flow is also carried out as an initial test of the described method. It is concluded that the experiences from the Sädva dam are valuable with regard to the use of the resistivity method on embankment dams. Resistivity monitoring data may be used to qualitatively assess the seepage through the dam. For quantitative assessment, the method is promising and the data from the Sädva dam constitute an interesting initial approach. However, many assumptions and simplifications are made and more work on refining the method is needed.

INTRODUCTION

There are approximately 25 000 registered large embankment dams, with a height exceeding 15 m, in the world. An ageing population of dams raises various questions regarding dam safety issues. In Sweden the average large dam was built in the late 1950s and the situation is similar in many other countries (ICOLD 2003).

For embankment dams the main safety concern is seepage. Methods for monitoring the seepage and for detecting internal erosion give essential information for the safety evaluation of earth embankment dams. Together with overtopping, internal erosion through the dam or the foundation is the most frequent reason for embankment dam failures (ICOLD 1995; Foster *et al.* 2000a). While overtopping scenarios might be difficult to predict, they are easier to perceive and monitor. An efficient monitoring system for internal erosion, on the other hand, is a far more complicated task.

* pontus.sjodahl@hydroresearch.se

Internal erosion in the embankment or in the foundation of the dam may reach an advanced stage before any sign is visible on the outside of the dam. The first indication may be higher seepage rates, a visually observable concentrated leak at the downstream toe or high turbidity in the seepage water. According to an inventory among Swedish dam owners, the most common method of detecting internal erosion processes in Swedish embankment dams has been through identification of sinkholes by visual inspection (Norstedt and Nilsson 1997). This inventory revealed that 27 Swedish dams had reported sinkholes ranging from 0.5 m in diameter to 15–30 m^3 in volume. In a subsequent study poor filter design was established as a reason for sinkholes in the majority of those dams (Nilsson *et al.* 1999). None of these incidents resulted in a dam failure. Recent research demonstrates that embankment dam failure caused by internal erosion may occur quite abruptly and the time between an early warning from a concentrated leak at the downstream toe to a full dam failure at the crest may be just a few hours (Foster *et al.* 2000b; Fell *et al.*

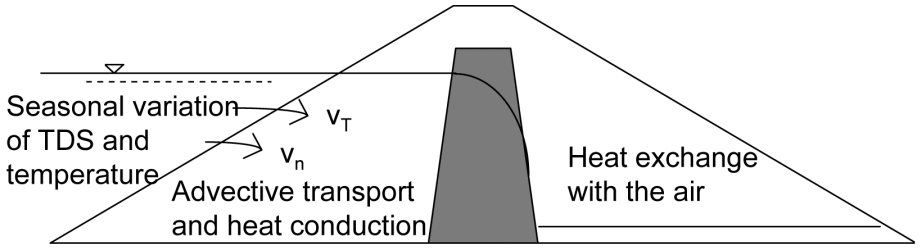

FIGURE 1
Cross-section of an embankment dam showing the important transport processes that affect the resistivity variation.

2003). Seepage monitoring systems with higher accuracy and improved spatial resolution are therefore of great value, since they may extend the critical time between an early warning and a potential dam failure.

The resistivity method is well established for a broad variety of purposes in engineering and environmental ground investigations. Long-term resistivity monitoring is an unconventional method for dam monitoring that may have the potential to detect anomalous seepage through embankment dams. The method is non-intrusive, which is a major advantage for use on existing dams. Leakage detection and structural status control of existing dams using the resistivity method have been tried on many occasions (e.g., Butler and Llopis 1990; Titov *et al.* 2000; Van Tuyen *et al.* 2000; Buselli and Lu 2001; Panthulu *et al.* 2001; Sjödahl *et al.* 2005; Song *et al.* 2005). A powerful approach is to carry out repeated measurements (Johansson and Dahlin 1996) or long-term monitoring (Johansson *et al.* 2005; Sjödahl *et al.* 2008). This approach of evaluating resistivity monitoring data is based on its time variation, which requires a fairly long investigation period to establish what is the normal resistivity variation, i.e., the seasonal variation due to temperature changes and reservoir level changes among other factors. Deviations from the established normal background are taken to indicate anomalous conditions in the dam.

In this paper an approximate method of estimating seepage from such long-term monitoring resistivity data is presented. The method is described in the next section. It is based on a number of simplified evaluation concepts (Johansson 1997) and was originally tested on occasional repeated measurements from another Swedish dam (Johansson and Dahlin 1996). The excellent data quality from the resistivity monitoring of the Sädva dam now allows for a more thorough evaluation on a dam with continuous long-term monitoring data. Identified inhomogeneities in the resistivity distribution along the Sädva dam are used as an example. Sädva was the second embankment dam to get a permanently installed resistivity monitoring system in an on-going Swedish research programme.

SEEPAGE INDUCED RESISTIVITY CHANGES

Embankment dams are constructed from earth and rock. These materials are permeable to a certain degree and therefore a steady seepage flow is the normal state of an embankment dam. The amount of seepage flow is restricted and mainly governed by the low permeability zone of the dam. In Swedish embankment dams this zone is commonly constructed out of glacial till. Increasing seepage flows is a dam safety concern as it may be associated with internal erosion.

All dams in their natural state experience some degree of seepage flow entering from the reservoir. The properties of the reservoir water will thus affect the inner part of the dam. Temperature and ion content are two characteristics of the seepage water that vary seasonally in the reservoir. The latter is commonly expressed as total dissolved solids. The seasonal variations in temperature and total dissolved solids in the reservoir water propagate with the seepage water and cause a time dependant resistivity variation inside the dam. These variations may therefore be a useful surrogate for tracking internal seepage water. As the resistivity of the soil is affected by temperature and ion content (measured as total dissolved solids), the signature of the seepage water may be observed in the inner part of the dam by repeated resistivity measurements.

The resistivity of the water has been shown empirically to depend on temperature according to equation (1), where ρ_T is the resistivity at temperature T and the temperature coefficient of resistivity α = 0.025° C^{-1} (Keller and Frischknecht 1966). Resistivity variation in the reservoir water that is not caused by temperature variations is assumed to originate from variations in total dissolved solids.

$$\rho_T = \frac{\rho_{18}}{\left(1+\alpha\left(T-18\right)\right)} \qquad \rho_{18} = \text{resistivity at } 18^\circ \text{ C} \qquad (1)$$

To fully describe the seepage-induced resistivity variation in the dam we have to consider a set of coupled transport processes for heat and solute. Heat conduction, mainly through the unsaturated parts of a dam, may also be important for low seepage flow rates and small dams. Water level variations and thermal stratification in the reservoir should also be considered. Geothermal flow may be important for large dams.

The seasonal variation of the resistivity in the reservoir water is separated into two parts when the seepage water passes through the dam. The solutes penetrate into the dam with the pore velocity v_n, while the temperature travels with the thermal velocity v_T (Fig. 1). The resistivity variation in the dam is therefore a combined result of these two transport processes, which are further described in this paper. Two models for the two separate transport processes are presented and compared. The first method analyses the time lag between the resistivity variation in the reservoir and inside the dam. It is a simplified one-dimen-

sional method. The velocity is obtained directly from the lag-time and the length of the seepage path. The second method assumes a concentrated seepage flow in a zone where the seepage flow is much higher than in the surrounding parts. These methods are described below. Both methods can be applied for separate analysis of temperature as well as total dissolved solids variation.

Temperature variations in embankment dams

The temperature in an embankment dam depends mainly on the temperature in the air and in the upstream reservoir. These temperatures vary seasonally and create temperature waves that propagate through the dam. At low seepage flow the seasonal temperature variation will be small. The influence from the air temperature at the surface decreases exponentially with depth and both theoretical calculations and field measurements indicate that the influence will be less than 1–2° C at 10 m depth and less than 0.1° C at 20 m depth for Swedish conditions (Johansson 1997). For the areas investigated in this paper, which are situated at 20 m depth, the influence from the air is therefore considered negligible. Any larger variation below this depth is caused by the seepage flow.

If substantial quantities of water seep through the dam, then the water temperature from the reservoir will influence the temperature inside the dam. At high seepage flow rates, the temperature variation of the water in the upstream reservoir completely determines the temperature inside the dam. The seasonal temperature variation in the dam is thus in practice directly proportional to the seepage flow rate.

The thermohydraulic behaviour of an embankment dam is complex. It includes such basic thermal processes as heat conduction (from the dam crest and from the foundation due to geothermal flow), advection and radiation. The first two processes are partly coupled to each other because viscosity and density are temperature dependent. This behaviour is further complicated by the variation in material properties in the dam and the different conditions in the saturated and unsaturated parts of the dam. In order to analyse the problem certain assumptions have to be made.

The influence of radiation consists of inflow from the sun or outflow to the atmosphere. This influence is restricted to the superficial part of the dam because of the short duration of the heat pulse, which is mainly controlled by the diurnal cycle. In the following analyses it is therefore assumed that the temperature inside the dam is independent of radiation. The geothermal flow is also ignored.

The energy flux consists of heat conduction in the solid phase and in the water, heat advection with the average seepage water flow and dispersion due to variability in the seepage water flow velocities. The energy balance equation can then in the general form be written as in equation (2).

$$C_0 \frac{\partial T}{\partial t} = \frac{\partial}{\partial x_i}\left(\lambda_0 \frac{\partial T}{\partial x_i} - C_w T q_i - Q_i^{disp} \right) \qquad (2)$$

C_0 = volumetric heat capacity of the soil (J/m^{3}K)
C_w = volumetric heat capacity of the water (J/m^{3}K)
Q_i^{disp} = energy flux due to mechanical and thermal dispersion (J/m^{2}s)
q_i = leakage flow (Darcy flow) (m/s or m^3/s per m^2)
T = temperature (° C)
t = time (s)
x_i = coordinate (m)
λ_0 = thermal conductivity of the soil (including solids, water and air) (W/mK)

The advective part of the energy flux is caused by the seepage water flow. From the second term on the right-hand side of equation (2), a thermal velocity v_T can, for the one-dimensional case, be written as in equation (3) (Claesson *et al.* 1985).

$$v_T = \frac{C_w}{C_0} q \qquad (3)$$

The thermal velocity describes the velocity of a thermal front through the dam. This velocity is similar but not identical with the velocity of the leakage water in the pore structure v_n, which depends on the porosity n ($v_n = q/n$).

Tracers can often be assumed to be conservative, travelling with the pore water velocity. The temperature also acts as a tracer but is travelling with the thermal velocity instead of the pore velocity. The temperature cannot be treated as a conservative tracer, as it also depends on heat conduction.

To solve equation (2) the flow q_i must also be calculated. This is done by using the mass conservation equation and the general form of Darcy's law, which gives the equation of motion for the leakage water flow in steady state conditions (equation (4)) (Bear 1979).

$$\frac{\partial}{\partial x_i}\left(k_{ij} \frac{\partial p}{\partial x_j} + \rho_f k_{ij} g_j \right) = 0 \qquad (4)$$

k_{ij} = permeability (m^2)
p = pressure (N/m^2)
ρ_f = fluid density (kg/m^3)
g_j = gravity (m/s^2)

This equation, with initial and boundary conditions, describes the seepage water flow induced by differences in pressure and by differences in density of the water. It should be observed that both the density and viscosity of the water are dependent on the temperature. A general solution of heat and water flow in a dam is based on equation (2) and equation (4) in combination with initial conditions and boundary conditions. The equations are coupled since equation (4) depends on the temperature field while the second and third terms in equation (2) depend on the flow field.

Lag-time method using the thermal velocity

The lag-time method can be applied in this case if the heat conduction perpendicular to the flow direction is ignored, i.e., a

one-dimensional approximation. The lag-time t_d is the time between the temperature pulse at the boundary $x = 0$ and the measured temperature variation at a point x. The velocity of the temperature wave is the thermal velocity. The thermal velocity is then obtained directly from the lag-time and the length of the seepage path, which is assumed to be equal to the distance between the boundary and measuring point x:

$$v_T = \frac{x}{t_d} \tag{5}$$

The assumption of no heat conduction perpendicular to the flow direction is valid for large seepage flows or for large seepage zone thicknesses, where the vertical heat exchange is negligible, particularly in the central part of the zone. Combining equations (3) and (5) gives an expression for the relation between the seepage flow and the lag-time (equation (6)).

$$q = \frac{C_0 x}{C_w t_d} \tag{6}$$

The seepage flow calculated in equation (6) is called q_T as it is related to the lag-time of the thermal velocity. It can now be calculated for known values of the volumetric heat capacity, which is assumed to be constant along the seepage path. Typical values for the volumetric heat capacity can be found in Sundberg *et al.* (1985).

The assumptions concerning heat transport are not valid for small leakage zones where the heat losses around the leakage zone can be large. The approximations are more valid for larger zones, with cross-sections of some 10 m^2 or more (Johansson 1997).

Concentrated seepage assuming temperature variation

An analytical model for the two-dimensional temperature field at a concentrated seepage flow was described by Johansson (1997). The most important assumptions in the model are:

- a sinusoidal temperature variation at the upstream boundary.
- seepage is limited to a zone of constant height.
- one-dimensional advection and vertical heat conduction in the central layer.
- only vertical heat conduction in the upper and lower layer.
- constant thermal properties in the layers.

These assumptions have generally been found to be valid for applications in embankment dams (Johansson 1997). The model is now incorporated in commercial software, which has been used for the calculations below (Johansson and Hellström 2001). The software presents the two-dimensional temperature field with input of seepage flow, thermal properties and geometrical data. Subsequently, the calculated temperature field is transformed to resistivity using equation (1), assuming constant total dissolved solids in the reservoir.

Lag-time method using the pore velocity

The variation of total dissolved solids in the water is assumed to act as a conservative tracer following the seepage flow through the dam as described by the well-known one-dimensional transport equation (equation (7)) given by Bear (1979).

$$\frac{\partial C}{\partial t} = D_h \frac{\partial^2 C}{\partial x^2} - \frac{q}{n}\frac{\partial C}{\partial x} \tag{7}$$

D_h is the coefficient of hydrodynamic dispersion and C is the concentration of the tracer. For the application of evaluating the time lag between the extreme values in the reservoir and inside the embankment dam, the dispersion term can be ignored. The velocity of the tracer will follow the pore velocity v_n, which depends on porosity n. Under such conditions, the temperature impact on the resistivity can be ignored and the seepage flow will be a function of only the porosity and the measured time lag, t_d (equation (8)).

$$q = \frac{nx}{t_d} \tag{8}$$

The seepage flow calculated in equation (8) is called q_{TDS} as it is related to the lag-time of the pore velocity, i.e., the velocity with which the total dissolved solids (TDS) in the water is assumed to travel.

The two estimated values of the seepage flow (q_{TDS} and q_{T}) can be interpreted as limits for the real seepage flow q since it can be proved that the pore velocity is larger than the thermal velocity for typical values of the thermal properties in the soil (equation (9)).

$$\frac{nx}{t_d} < q < \frac{C_0 x}{C_w t_d} \tag{9}$$

If typical values of n, C_0 and C_w are inserted in equation (9), limits are specified for practical applications (equation (10)).

$$0.2 < \frac{q t_d}{x} < 0.6 \tag{10}$$

These limits do not include the entire range of uncertainty values. In many cases it is difficult to estimate the length of the real seepage path as well as the lag-time. Dispersion will not influence the lag-time but it strongly affects the temporal variations of the resistivity and complicates the evaluation of the lag-time. However, in the absence of more accurate methods, such limits may sometimes be good enough to estimate the seepage flow in dams. The relation between these velocities can be expressed (equation (11)). Typical values for soils used in embankment dams indicate that tracers, such as total dissolved solids, will pass approximately twice as fast as the thermal front.

$$v_T = \frac{C_w}{C_0} n v_n \tag{11}$$

SÄDVA EMBANKMENT DAM

The Sädva dam is located in the upper part of the Skellefteälven River just south of the Arctic Circle. It has a reservoir storage

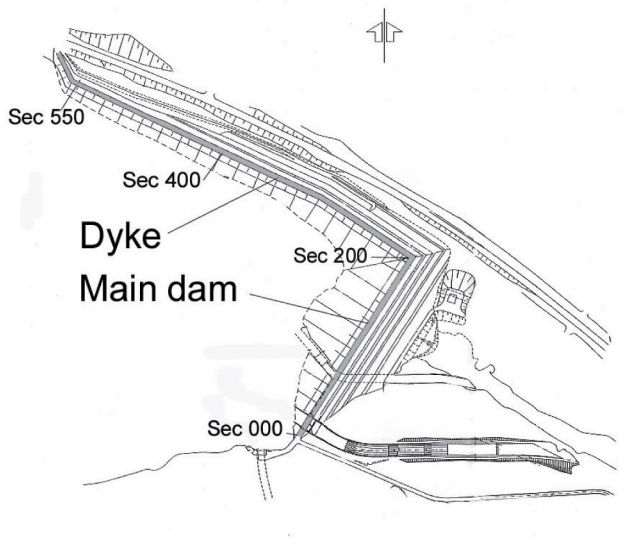

FIGURE 2
Plan of Sädva dam. The 210 m long main dam is crossing the river channel and the 410 m long dyke extends along one side of the river channel. Sec refers to dam section in metres.

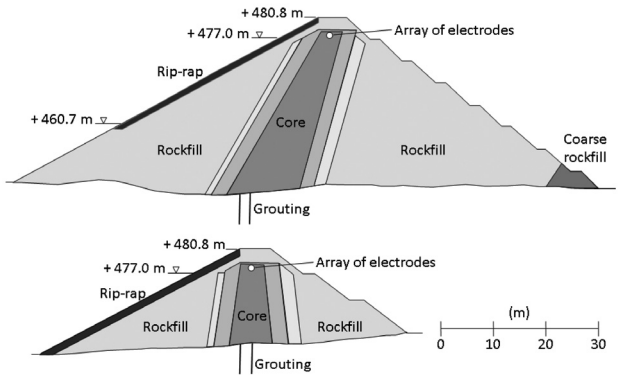

FIGURE 3
Principal cross-section of the main dam (top) and the dyke (bottom). A rockfill dam with filter zones surrounding the central core of glacial till. Rip-rap on the upstream face (left side) protects the dam from surface erosion.

volume of 625 million m^3. The dam and power plant was put into operation in 1985. The total length of the dam is 620 m, which is divided into a 210 m long main dam across the old river channel and a 410 m long dyke along the old river channel (Fig. 2). The maximum height of the main dam is 32 m but considerably lower for the dyke averaging around 10 m. Both dams are zoned rockfill embankment dams with a central core of fine-grained glacial till (Fig. 3). Annual water level variations are around 16 m (+460.7 to +477.0 m.a.s.l.), which is half the height of the main dam. The high variations constitute a complication in the evaluation of the measurements but at least the seasonal pattern is roughly the same from one year to another (Fig. 4). The reservoir reaches its highest level in autumn and is lowered during the winter to its lowest levels and is filled up again during early summer by the vast snowmelt. The main dam is founded on bedrock, while the dyke is founded on moraine except where it connects to the main dam.

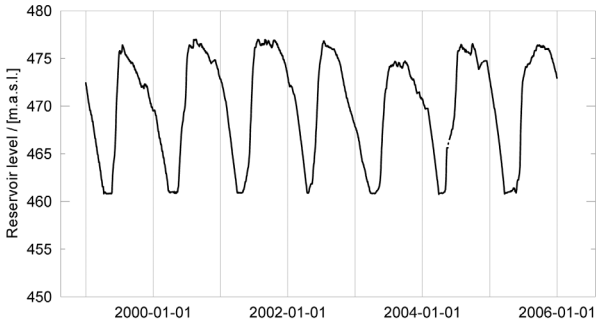

FIGURE 4
Reservoir levels at Sädva dam. The retention levels are at 460.7 and 477.0 m.a.s.l. The reservoir is emptied during winter and rapidly filled during the snowmelt period in early summer.

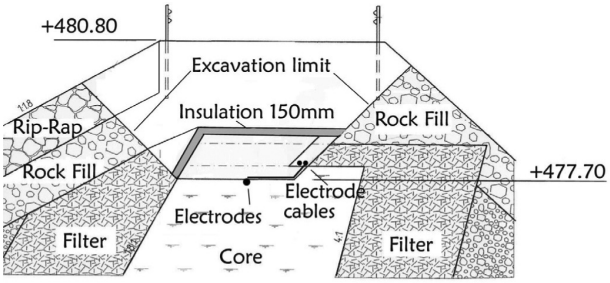

FIGURE 5
Installation of electrodes and cables along the dam crest. The electrodes were installed into the top part of the dam core 3.1 m below the dam crest.

In accordance with new Swedish guidelines for floods it was decided to increase the height of the core by 0.7 m and to construct an additional spillway. This was done in 1999. Since the crest was excavated down to the core during this work, a unique possibility arose to install monitoring equipment and it was decided to use the dam as a research dam for dam monitoring.

A correct electrode type and a proper installation are fundamental for all electric measurements. Based on the experience from the Hällby dam (Johansson and Dahlin 1998; Johansson *et al.* 2005) it was decided to use stainless steel electrodes for the resistivity measurements. It was also decided to install non-polarizable electrodes for self-potential (SP) measurements on the main dam. The electrodes were installed on the original core crest, about 3.1 m below the dam crest (Fig. 5). An insulation layer was placed on the top of the core to prevent it from freezing. The resistivity electrodes consist of 0.25 m × 0.25 m stainless steel plates. The electrodes are connected to polyurethane covered stainless steel wires, which are joined to cable splits (pig-tail splits) on a polyurethane covered multi-core cable. The non-polarizable copper-copper sulphate electrodes are joined to

a multi-core cable in the same way as the steel plate electrodes. These electrodes were delivered pre-packaged in a cloth bag filled with a bentonite mix designed to give good coupling to the surrounding soil.

In total, 128 electrodes were installed. An electrode spacing of 6 m for the steel plate electrodes was chosen for the entire dam. The non-polarizable electrodes were installed only on the main dam, with a spacing of 6 m but shifted 3 m relative to the steel plate electrodes, giving 3 m electrode spacing on the main dam. Special measurement protocols were designed to avoid using the non-polarizable electrode as current electrodes. A data acquisition system for automatic measurements of resistivity and SP data was installed in 2001. It was designed to make daily measurements using the electrodes installed on the crests of the main dam and the dyke, as well as temperature and resistivity measurements in the reservoir water via two probes. The Sädva dam and its installations are thoroughly described in earlier reports (Dahlin *et al.* 2001; Johansson *et al.* 2005).

RESISTIVITY MEASUREMENTS

Data acquisition was carried out using a modified version of the ABEM Lund Imaging System, which is a multi-electrode data acquisition system for resistivity surveying (Dahlin 1993, 1996). Daily measurements of resistivity and SP are automatically carried out at the electrodes along the crests of the main dam and the dyke but only resistivity data are presented here. The data acquisition process is completely controlled by the software, whereby the software scans through the measurement protocols selected by the user. A number of configurations have been tested. Currently, Wenner array, dipole-dipole array, pole-dipole array and gradient array are running in the monitoring programme. Reciprocal measurements have also been carried out to assess measurement errors. Preliminary evaluation of the data quality has been done by calculating the measurement errors from the difference between normal and reciprocal measurements (Dahlin *et al.* 2001). Reciprocal measurements are carried out by using the potential electrodes for transmitting current and vice versa. In theory this should give identical results and differences are due to measurement errors (Parasnis 1997). Resulting estimated measurement errors are below 1% for proper instrument settings, which indicate good data quality and stable conditions. Reciprocal measurements were added to the monitoring setup in later years and such data are not available for the first years.

The fresh waters of northern Scandinavia generally have high resistivities and the Sädva reservoir is no exception. Daily measurements of temperature and resistivities of the reservoir water (Fig. 6) are taken by a submersible probe mounted on the concrete structure of an old spillway. Equation (1), with $\alpha = 0.025^{\circ}\,C^{-1}$, is used to normalize for temperature. Furthermore the Swedish University of Agricultural Sciences (SLU) carries out monthly measurements of the water chemistry in Slagnäs approximately 100 km downstream in the river system. These measurements are reported as electrical conductivity (inverse of

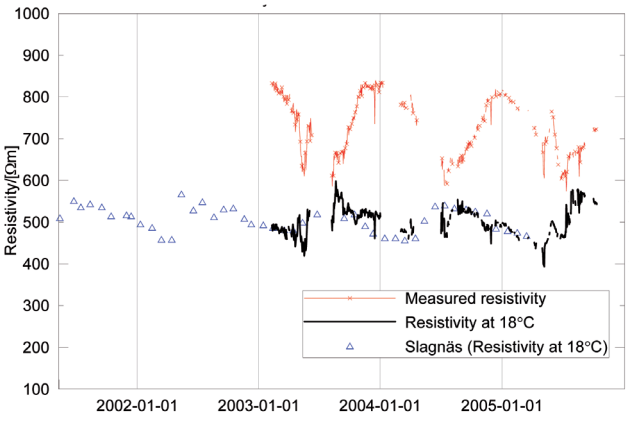

FIGURE 6
Resistivity in the Sädva reservoir and monthly measurements from Slagnäs approximately 100 km downstream (SLU 2005).

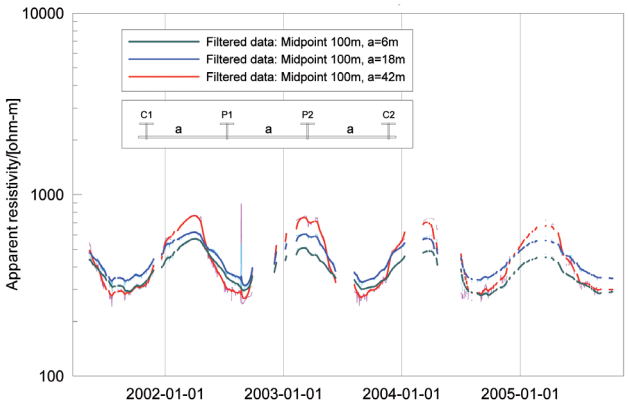

FIGURE 7
Time series of apparent resistivities for a measurement configuration with the midpoint located at chainage 100 m and three selected electrode separations, a, representing different pseudodepths. C1 and C2 are current electrode positions and P1 and P2 are potential electrodes for the measurement configurations.

resistivity) at 25º C and have been transformed to resistivity at 18º C using the same relationship. The different measurements correlate well considering that they are carried out using different equipment and are measured at locations 100 km apart in the river (Fig. 6). It is clear that even after normalizing for temperature dependence there is a seasonal variation in the resistivity of the reservoir. This variation consists of a rapid increase in resistivity in spring or early summer coinciding with the snowmelt period.

Plotted time-series of apparent resistivities are valuable for data quality analysis and to assess the performance of time-based data filtering. Data from some specific configurations, representing single points in the pseudosections, have thus been examined for the full monitoring period (Fig. 7). The straight lines in Fig. 7 represent filtered data. The processing routines for embankment

monitoring data were first developed at the Hällby dam, the first Swedish dam to get a permanent resistivity monitoring installation. At Hällby, special treatment of the data was needed due to problems with data quality. For this reason de-spiking and low-pass filtering methods have been implemented in the data processing routines to filter the data before inverse modelling is carried out (Johansson *et al.* 2005; Sjödahl *et al.* 2008). Filter parameters were adjusted to remove peaks successfully without disturbing the natural variations.

Quantitative evaluation of apparent resistivities is unsuitable since different electrode arrays have different sensitivity distributions both along the line and with depth that will give misleading information. Inverse numerical modelling (inversion) is therefore used to estimate the actual resistivity distribution in the investigated volume. Prototype software has been developed that automatically goes through the combined automatic routines for handling data from long monitoring periods. These routines include filtering of data, inverting data and finally presenting some statistical parameters for the whole period. Inversion of the filtered apparent resistivity data was done using the software Res2dinv version 3.54r (Loke 2004). This is a well-established routine for fitting of a number of surface measurements, i.e., apparent resistivities, to a model of subsurface resistivities. The theory has been described in literature (Loke and Barker 1995, 1996; Farquharson and Oldenburg 1998). Specifically the L1-norm optimization method (Claerbout and Muir 1973) was used in combination with the use of time-lapse inversion (Loke 2001) for the repeated data sets. Measurement errors were not integrated in the inversion process, due to lack of reciprocal data sets for the entire monitoring period, although this would have been desirable in order to optimize resolution and avoid artefacts (LaBrecque *et al.* 1996). More details about the methodology regarding measurements, treatment of the apparent resistivity and time-lapse inversion of the data are given in earlier reports (Johansson *et al.* 2005; Sjödahl *et al.* 2008).

The inversion approach used is based on a two-dimensional (2D) assumption, i.e., there is no variation in resistivity perpendicular to the electrode layout, which is clearly not valid for embankment dams when measurements are taken along the dam crest. The embankment dam geometry results in so-called 3D effects in the inversion, which distorts model resistivity values and depth location, as Sjödahl *et al.* (2006) demonstrated through numerical modelling. The modelling also showed that monitoring with an electrode layout along the crest of the dam is the most efficient approach for detecting changes inside the core of the dam with a single layout (Sjödahl *et al.* 2006). For many embankment dams in Sweden installation along the crest of the dam is the only practical option and layouts for 3D inversion are impossible to install due to site conditions. Since the data acquisition is carried out along a single line 2D inversion remains the only option and the results must be evaluated with this in mind and should in many cases be used as anomaly indicators to highlight where special attention and follow-up with other methods is called for. At Sädva, the 3D effects are expected to be severe for

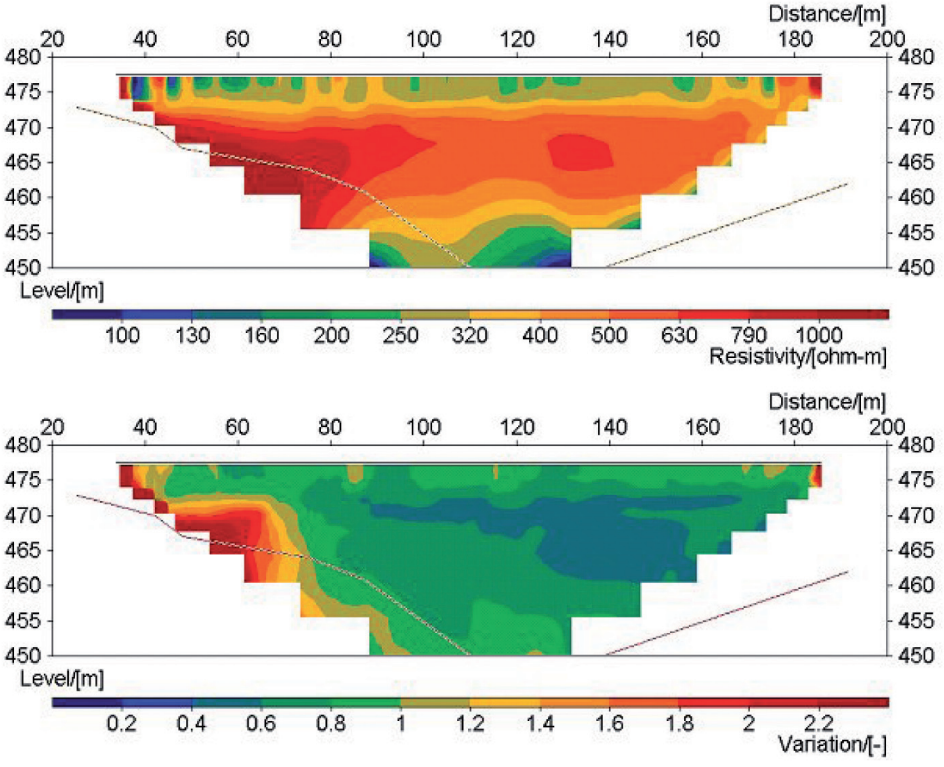

FIGURE 8
Sädva main dam longitudinal model sections with foundation level indicated (solid line). Medium inverted model of resistivity distribution (top) and relative variation ((ρ_{max} – ρ_{min}) / ρ_{median}) of inverted resistivity models (bottom), over the period from 12 May 2001 to 25 November 2005.

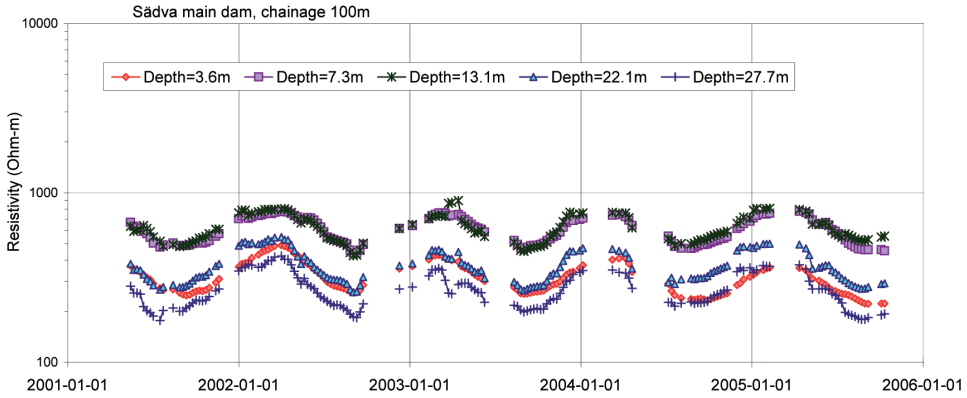

FIGURE 9
Time series of inverted resistivities from the main dam. Five different depths are represented, from the chainage 100 on the main dam.

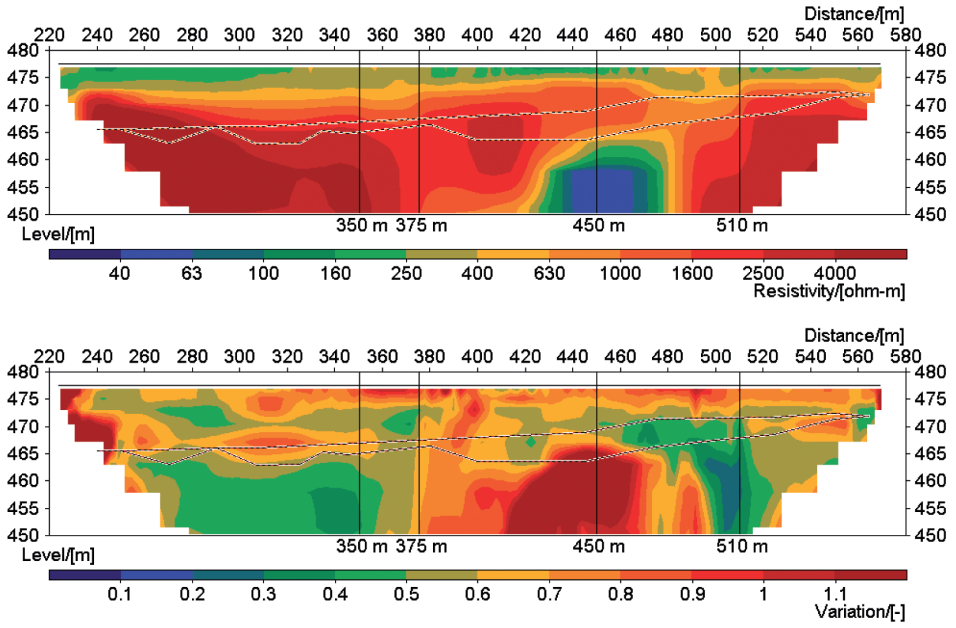

FIGURE 10
Sädva dyke longitudinal model sections with foundation and bedrock level indicated (solid lines). Medium inverted model of resistivity distribution (top) and relative variation (($\rho_{max} - \rho_{min}$) / ρ_{median}) of inverted resistivity models (bottom), over the period from 20 September 2001 to 25 November 2005. The four investigated areas at 350 m, 375 m, 450 m and 510 m are marked out.

the main dam. For the dyke the 3D effects should be smaller as it is lower and for the deeper parts of the models that cover the ground below the foundation of the dam, the distortion is judged to be of less importance.

Results from the Sädva main dam over the period from 12 May 2001 to 25 November 2005 are presented (Fig. 8). This whole evaluation period was divided in 7-day periods and one inverted model was created for each such 7-day period. The upper part of Fig. 8 is the median of those models and represents an overview of the spatial resistivity distribution. Anomalous zones are of interest and not much attention is paid to absolute values in the interpretation of data due to the previously mentioned distortion.

The lower part of Fig. 8 represents the relative variation, calculated as ($\rho_{max} - \rho_{min}$) / ρ_{median}, of the 7-day data sets. This is a very rough statistical measure but serves reasonably well as a tool for indication of zones with high amplitudes in the seasonal resistivity pattern, which is the main interest.

By evaluating the median resistivity model and the relative variation of the inverted models, anomalies in space and time respectively are identified. These two concepts are fundamental for interpretation of resistivity monitoring data.

In general, the conditions on the main dam have been found to be homogeneous with stable variations. The resistivity distribution and the variations are consistent along the full length of the dam except for an area immediately next to the spillway structure at the left end of the section (Fig. 8), which contrary to standard dam praxis is viewed from the downstream side. This anomaly is probably an effect from the spillway structure but it is worth keeping in mind that the area adjacent to a concrete structure is a common problem area due to lower compaction of the core. However, in this case, there are no other observations indicating increased seepage or other reported problems with the dam.

More detailed investigations of the variations in selected areas can be performed by studying the resistivity over time in specific parts of the dam. An example of such a time-series for the

Sädva main dam at chainage 100 m is given in Fig. 9. The obvious seasonal variation is a consequence of the changing water level and seepage-induced variations due to the resistivity variation of the reservoir water. The variations are smooth and stable, which indicates that the dam is performing well. There are no signs of unusually high resistivity variations, increasing resistivity variations or long-term trends of increasing resistivity as have been seen at the Hällby dam (Sjödahl *et al.* 2008). Such phenomena might be taken to indicate high seepage levels, increasing seepage and internal erosion respectively.

Monitoring data from the Sädva dyke over the period from 20 September 2009 to 25 November 2005 are presented here (Fig. 10). Evaluation has been done in the same manner as for the main dam.

The conditions on the dyke are not as homogeneous as for the main dam. The most obvious difference is the large diversity in the foundation, which is probably due to variation in rock type or rock quality in the underlying rock. However, the clearly higher relative variation in the same area is an indication of the presence of a possible seepage path in the foundation. The resistivities inside the dyke itself are generally higher than in the main dam. Moreover, for the dyke there is considerable variation in resistivity along the dam (Fig. 10, top) compared with the homogeneous conditions in the main dam. This can be explained by larger variations in material properties in the dyke. The relatively low variations inside the dyke (Fig. 10, bottom), indicate that the dyke is performing reasonably well. However, the possible seepage path in the foundation is worth some more attention and will be examined in the next section.

SEEPAGE EVALUATION

The resistivity variation in the dam is dependent on the seepage flow as described above. However in field applications other factors may also be of importance.

One such factor is the water level variation, which is clearly significant at Sädva. Numerical modelling has shown that water level changes on the order of half the reservoir height may cause resistivity changes of up to 40 per cent in apparent resistivity data (Sjödahl *et al.* 2006). No further detailed modelling, nor any particular attempt to correct this effect at the Sädva dam, have been carried out in this initial study. However, the effect is reduced by the fact that the studied areas within the dam are situated below the reservoir level throughout the year.

Another complicating factor at Sädva is that the resistivity variation is affected by both total dissolved solids and temperature, with neither factor clearly dominating the resistivity variation. As a result, some of the assumptions of the evaluation methods will not be fulfilled and the evaluation becomes more complicated. Nevertheless significant differences in resistivity and in the characteristics of the resistivity variation were found when comparing different locations along the dam. Therefore comparing these parts gives a qualitative assessment of the status of different parts of the dam. However when evaluating seepage conditions in some areas quantitatively, the disturbance from water-level changes and interacting temperature and total dissolved solids variation become troublesome.

Qualitative evaluation

Four different areas have been selected for seepage evaluation. The areas are all situated at the same depths at different distances along the dam. The chainages at 350 m, 375 m, 450 m and 510 m, as marked in Fig. 10, have been selected for testing of the seepage evaluation methods. A single level (+458 m.a.s.l.) has been selected. This is below the low water retention level, meaning the soil will be saturated throughout the year. The dam geometry is also almost identical in all areas, so a similar resistivity variation should be expected at all four areas if they all have seepage flow regimes. The first evaluation step is just to compare those areas qualitatively, based on the result shown in Fig. 11.

The area with the smallest resistivity variation is at chainage 510 m, where the annual variation is only about 12%. No clear seasonal variation is found although there seems to be higher values in the autumn than in spring. The effect may just be caused by the changes in the water level and the seepage flow must then be very small.

The largest resistivity variation along the dyke is at chainage

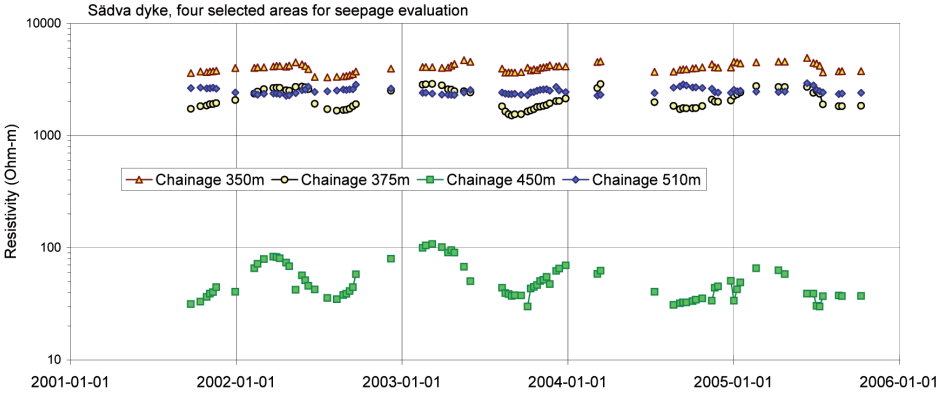

FIGURE 11
Four selected areas for seepage evaluation. All areas from depth 20 m, corresponding to 458 m.a.s.l.

TABLE 1

Estimated seepage from measured time-lag at Ch 350, 375 and 450 assuming that the maximum resistivity in the reservoir occurs on Dec 15th and minimum on Aug 1st. The length between inflow and measuring cell is assumed to be 20 m and the porosity 0.2. The volumetric heat capacity is 4.2 MJ/m^3/K for water and 2.5 MJ/m^3/K for soil

CH		2002	2003	2004	2005	Mean	td (days)	qTDS (10-6 m/s)	qT (10-6 m/s)
350	t(Rmin)	17 Aug	21 Jul	1 Aug	17 Jul	29 Jul	363	0.13	
	t(Rmax)	12 May	18 May		12 Jun	24 May	160	0.29	
375	t(Rmin)	11 Aug	31 Aug	5 Sep	28 Aug	26 Aug	391	0.12	
	t(Rmax)	7 Apr	9 Mar	14 Mar	20 Feb	13 Mar	88	0.52	
450	t(Rmin)	11 Aug	7 Sep	22 Aug	17 Jul	14 Aug	378	0.12	0.36
	t(Rmax)	24 Mar	9 Mar		20 Feb	8 Mar	83	0.56	1.65

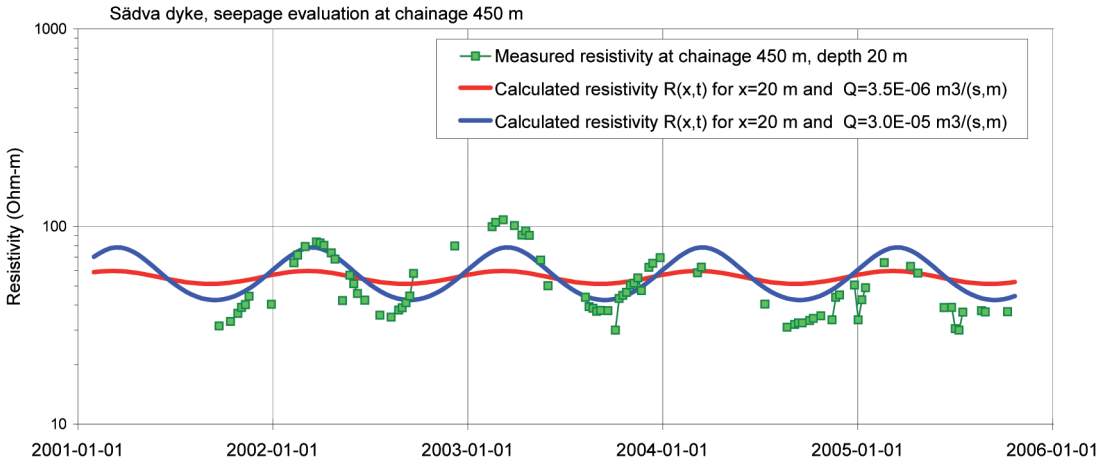

FIGURE 12

Seepage evaluation at chainage 450 m on the Sädva dyke. Measured resistivities on 20 m depth (458 m.a.s.l.) and calculated variations from two different seepage flow rates. The calculations represent the temperature change from seepage-induced temperature variations, which are transformed into resistivity variation using equation (1). The curves are then shifted in parallel to oscillate around the mean value of the measurements.

450 m, with an annual variation about 75%. The shape of the curve is similar to a sine wave, indicating a thermal response and thus significant seepage flow. A perfect sine wave is not to be expected at this location close to the Arctic Circle, where the water temperature is around zero for 6–8 months and reaches approximately 14° C in the summer. In addition the variation in the water level causes varying conditions, which will also deform the sine wave response in the dam.

The resistivity variation in the remaining two areas, chainage 350 m and chainage 375 m, exhibit variations with appearances somewhat in-between the above mentioned but more similar to the variation in chainage 510 m. The annual variation at chainage 350 m is 19% and at chainage 375 m it is 32%. From visual observation of the curves, the variation is less reminiscent of a sine wave response. In particular the slower rise and steeper lowering of these curves indicates influence from the typical variation pattern of the total dissolved solids and the temperature effect is smaller and thus the seepage flow is lower. The resistivity variation is mainly affected by total dissolved solids variation.

Quantitative evaluation

Apart from qualitative judgements, as presented above, quantitative estimations may also be performed. For this purpose, the data from the examined areas can be used to estimate the seepage flow rate using the lag-time methods (equations (6) and (8)) and the software for concentrated flow as described previously. The characteristic data as well as the seepage flow rates for each area are summarized in Table 1. The last two columns represent the seepage rates calculated from equations (6) and (8) using the lag-time methods. As shown in equation (9), these values can be interpreted as the lower and upper limits of the real seepage flow. The lowest flow rates are found in chainage 510 m and they are in the order of 10^{-7} m^3/s per m, which is just a few drops per square metre per second. Such low flow rates indicate that the integrity of the dam and the foundation is fully satisfying. The highest value at chainage 450 m is about 10^{-6} m^3/s per m. This flow, even though it is ten times higher than in chainage 510 m, is actually also low and fully acceptable. The total seepage in the low-resistivity area around chainage 450 m, about 30 m long and

10 m high, will only be about 0.3 l/s. Such small flow rates will be difficult to detect using conventional methods, such as a seepage weir collecting water over some hundred metres along the dam. These low flows are also well below any reasonable seepage alarm level and at the moment they form no threat to the safety of the dam. Seepage rates need to be at least 100 times higher or increasing to constitute a dam safety concern.

The result at chainage 450 m indicates that the concentrated seepage zone approach could be used. However in this case we must also assume that total dissolved solids is constant. The resistivity variation for two seepage flow rates was calculated using the software in Johansson and Hellström (2001) by transforming the calculated temperature response into resistivities using equation (1) and superposing it on an assumed resistivity level corresponding to the mean resistivity at chainage 450 m. The resistivity then shows a maximum value at the beginning of March (Fig. 12). The calculated variation is smaller than the measured variation, probably due to the influence from the total dissolved solids variation in the reservoir water. It is also clear that for the studied area the best agreement is found for a total seepage flow of 3.0×10^{-5} m^3/s per m. The assumed seepage zone height was 10 m for these calculations, which results in a seepage flow of 3×10^{-6} m/s, which is about three times higher than the value estimated from the 1D transport approach in Table 1.

Although these calculated flow rates are based on several simplified assumptions the results are useful for a dam owner, since they provide knowledge of at least the order of magnitude of the seepage flow rate in absolute values. However of more importance is the fact that the method allows detection of small relative changes both in time and in space, because any seepage increase may be of large importance. The early detection of a trend of increasing seepage is of great value for the overall safety of a dam.

CONCLUSIONS

The on-going monitoring programme, with daily resistivity measurements since 2001, at the Sädva embankment dam is a valuable experience for the application of the resistivity method on embankment dams. The following conclusions can be drawn from the installation and the measurements:

- Good electrode contact was achieved at the installation and the measured data exhibit low noise levels. For central core dams, installation of the electrodes inside the upper part of the dam core can be an efficient way to avoid data quality problems due to high electrode contact resistance.
- A partially automatic method of handling long time-series resistivity data has been developed. This evaluation is based on identifying zones with i) long-term changes in resistivities, ii) high resistivity variations and iii) increasing resistivity variations. The method is efficient and useful.
- The 2D inversion models must be assessed with the distortions due to geometry in mind and the method may therefore in many cases be used as an anomaly detector rather than a tool to measure the true resistivity variation. Along dams with a constant cross-section, zones with anomalous behaviour require special attention and follow-up investigations.
- Seasonal resistivity variations are obvious, both in the embankment dam and in the reservoir.
- The resistivity structure and the distribution of the resistivity variation within the main dam are rather homogeneous, except for a zone immediately next to the spillway.
- There is a large variation in the resistivity structure of the dyke with a low resistivity zone that also exhibits large variations with time. As the dyke is low in relation to the depth of this structure and almost constant in cross-section, it is interpreted as a zone of anomalous material properties within the foundation of the dyke. The distribution of the resistivity variation within the dyke, i.e., at shallower depth, is higher than the main dam, although the levels are not notably high.

In addition to reporting resistivity monitoring data, methods for evaluating seepage on embankment dams are presented along with initial attempts to apply these methods on four selected locations on the Sädva dam. The following conclusions can be drawn from this part of the work:

- Methods for evaluation of seepage in embankment dams from resistivity data are theoretically described. The methods are based upon the seasonal variation of temperature and total dissolved solids in the reservoir. The signature of this variation propagates with the seepage water from the reservoir downstream through the inner parts of the dam. Resistivity is affected by both temperature and total dissolved solids and it is assumed that this signature can be measured by the resistivity monitoring system.
- Qualitative assessments of the seepage situation in the dam can be carried out by comparing different chainages along the dam. This is a useful method for detecting weaker zones along the dam. It is less challenging but also less informative than the quantitative assessment.
- The quantitative assessment is an unconventional method to estimate seepage flow in different parts of the embankment dam. Even if many assumptions and generalizations are used for the quantitative approach it must be remembered that there are no other available methods that are able to perform such measurements. This method can estimate seepage flow without knowledge of the hydraulic conductivity inside the embankment, which is advantageous as this parameter is particularly difficult to measure. Moreover, for the practical applications there is plenty of room for engineering simplification, because knowledge of seepage flows with an accuracy of an order of magnitude is of great value for most dam owners. The results from Sädva are promising as an initial effort but more work is clearly needed for refinement of the method.

Finally, there are no indications from these observations that question the overall safety of the Sädva embankment dam. However, the zones with high resistivity variations will be kept under special observation in the future.

ACKNOWLEDGEMENTS

The work presented here was carried out with funding from Elforsk, Svenska Kraftnät and the Dam Safety Interest Group (DSIG). Skellefteälvens Vattenregleringsföretag AB, who owns Sädva dam, has given additional funding and valuable support.

REFERENCES

Bear J. 1979. *Hydraulics of Groundwater*. McGraw-Hill. ISBN 0070041709.

Buselli G. and Lu K. 2001. Groundwater contamination monitoring with multichannel electrical and electromagnetic methods. *Journal of Applied Geophysics* **48**, 11–23.

Butler D.K. and Llopis J.L. 1990. Assessment of anomalous seepage conditions. In: *Investigations in Geophysics No. 5: Geotechnical and Environmental Geophysics, Vol. II* (ed. S.H. Ward), pp. 153–173. SEG.

Claerbout J.F. and Muir F. 1973. Robust modeling with erratic data. *Geophysics* **38**, 826–844.

Claesson J., Eftring B., Eskilson P. and Hellström G. 1985. *Markvärme – En handbok om termiska analyser* (Ground Heat Systems – A Handbook on Thermal Aanalyses). Swedish Council for Building Research, Reports T16-T18. ISBN 9154044618, 9154044634, 9154044650 (in Swedish).

Dahlin T. 1993. *On the automation of 2D resistivity surveying for engineering and environmental applications*. PhD thesis, Lund University.

Dahlin T. 1996. 2D resistivity surveying for environmental and engineering applications. *First Break* **14**, 275–283.

Dahlin T., Sjödahl P., Friborg J. and Johansson S. 2001. Resistivity and SP surveying and monitoring at the Sädva embankment dam, Sweden. *Proceedings of the 5th European ICOLD Symposium,* 25–27 June 2001, Geiranger, Norway, pp. 107–113.

Dahlin T., Sjödahl P. and Johansson S. 2005. Resistivity monitoring for internal erosion detection at Hällby and Sädva embankment dams. *Proceedings of the International Symposium on Dam Safety and Detection of Hidden Troubles of Dams and Dikes*, 1–3 November 2005, Xi'an.

Farquharson C.G. and Oldenburg D.W. 1998. Applied geophysical inversion. *Geophysical Journal International* **134**, 213–227.

Fell R., Wan C.F., Cyganiewicz J. and Foster M. 2003. Time for development of internal erosion and piping in embankment dams. *Journal of Geotechnical and Geoenvironmental Engineering* **127**, 307–314.

Foster M., Fell R. and Spannagle M. 2000a. The statistics of embankment dam failures and accidents. *Canadian Geotechnical Journal* **37**, 1000–1024.

Foster M., Fell R. and Spannagle M. 2000b. A method for assessing the relative likelihood of failure of embankment dams by piping. *Canadian Geotechnical Journal* **37**, 1025–1061.

ICOLD 1995. *Dam Failures Statistical Analysis*. International Commission on Large Dams (ICOLD), Bulletin 99.

ICOLD 2003. *World Register of Dams*. International Commission on Large Dams (ICOLD), Paris.

Johansson S. 1997. *Seepage monitoring in embankment dams*. PhD thesis, Royal Institute of Technology, Stockholm.

Johansson S. and Dahlin T. 1996. Seepage monitoring in an earth embankment dam by repeated resistivity measurements. *European Journal of Engineering and Environmental Geophysics* **1**, 229–247.

Johansson S. and Dahlin T. 1998. Seepage monitoring in Hällby embankment dam by continuous resistivity measurements. *The 8th Congress of the International Association for Engineering Geology and the Environment*, Vancouver, pp. 95–102.

Johansson S., Friborg J., Dahlin T. and Sjödahl P. 2005. Long term resistivity and self potential monitoring of embankment dams – Experiences from Hällby and Sädva dams, Sweden. Elforsk Report 05:15 (available at www.elforsk.se).

Johansson S. and Hellström G. 2001. Software package for evaluation of temperature field in embankment dams. Manual for the software DamTemp ver 1.0 (available at http://www.hydroresearch.se).

Keller G.V. and Frischknecht F.C. 1966. *Electrical Methods in Geophysical Prospecting*. Pergamon Press.

LaBrecque D.J., Miletto M., Daily W., Ramirez A. and Owen E. 1996. The effects of noise on Occam's inversion of resistivity tomography data. *Geophysics* **61**, 538–548.

Loke M.H. 2001. Constrained time-lapse resistivity imaging inversion. *Proceedings of the Symposium on the Application of Geophysics to Engineering and Environmental Problems*, SAGEEP, Denver, Colorado, 4–7 March 2001.

Loke M.H. 2004. Rapid 2-D resistivity & IP inversion using the least-squares method, Manual for Res2dinv, version 3.54 (www.geoelectrical.com).

Loke M.H. and Barker R.D. 1995. Least-squares deconvolution of apparent resistivity pseudosections. *Geophysics* **60**, 1682–1690.

Loke M.H. and Barker R.D. 1996. Rapid least-squares inversion of apparent resistivity pseudosections by a quasi-Newton method. *Geophysical Prospecting* **44**, 131–152.

Nilsson Å., Ekström I. and Söder C.O. 1999. Inre erosion i svenska dammar. Elforsk report 99:34 (available at www.elforsk.se) (in Swedish with English summary).

Norstedt U. and Nilsson Å. 1997. Internal erosion and ageing in some of the Swedish earth- and rock-fill dams. *Proceedings of the 19 Congress of the International Commission on Large Dams (ICOLD)*, Florence, Italy.

Panthulu T.V., Krishnaiah C. and Shirke J.M. 2001. Detection of seepage paths in earth dams using self-potential and electrical resistivity methods. *Engineering Geology* **59**, 281–295.

Parasnis D.S. 1997. *Principles of Applied Geophysics*. Chapman & Hall ISBN 0412640805.

Sjödahl P., Dahlin T. and Johansson S. 2005. Using resistivity measurements for dam safety evaluation at Enemossen tailings dam in southern Sweden. *Environmental Geology* **49**, 267–273.

Sjödahl P., Dahlin T. and Johansson S. 2008. Resistivity monitoring for leakage and internal erosion detection at Hällby embankment dam. *Journal of Applied Geophysics* **65**, 155–164.

Sjödahl P., Dahlin T. and Zhou B. 2006. 2.5D resistivity modeling of embankment dams to assess influence from geometry and material properties. *Geophysics* **71**, 107–114.

SLU 2005. Databank för vattenkemi (Water chemistry database). Swedish University of Agricultural Sciences (available at http://www.ma.slu.se). (in Swedish)

Song S.H., Song Y.H. and Kwon B.D. 2005. Application of hydrogeological and geophysical methods to delineate leakage pathways in an earth fill dam. *Exploration Geophysics* **36**, 92–96.

Sundberg J., Thunholm B. and Johnsson J. 1985. *Värmeöverförande egenskaper I svensk berggrund* (Thermal Properties of Swedish Rock). Swedish Council for Building Research, Report R97:1985. ISBN 9154044464. (in Swedish)

Titov K., Lokhmanov V. and Potapov A. 2000. Monitoring of water seepage from a reservoir using resistivity and self polarization methods: Case history of the Petergoph fountain water supply system. *First Break* **18**, 431–435.

Van Tuyen D., Canh T. and Weller A. 2000. Geophysical investigations of river dikes in Vietnam. *European Journal of Environmental and Engineering Geophysics* **4**, 195–206.